Cracking in Spot Welding Aluminum Alloy AA5754

Cracking and its mechanisms during the resistance spot welding of aluminum alloys are analyzed

BY J. SENKARA AND H. ZHANG

ABSTRACT. The phenomenon of cracking was observed during resistance spot welding a commercial aluminum alloy AA5754, and mechanisms of cracking and healing are discussed in this paper. Metallographic study of welded coupons revealed cracks located on only one side of a weldment in the heat-affected zone (HAZ), with respect to the welding sequence. Cracks are visible from longitudinal cross sections only. Some of them are partially or fully filled. Crack appearance and orientation are fairly repeatable and their intergranular characteristics and dendritic fracture surface morphology prove they were formed at elevated temperatures in the presence of liquid metal. The discussion of metallurgical factors considering the Al-Mg equilibrium phase diagram and the possible temperature histories of various zones in a weldment during spot welding elucidated the approximate conditions for cracking during spot welding and for mending the structure. A thermomechanical analysis revealed a high possibility for tensile stress buildup on the cracked side of the weldments as a result of material flow, thermal stress development and localized straining.

Introduction

Aluminum-based alloys have been widely used in automobile structures due to their unique properties, such as high specific strength. Although large-scale production of aluminum-intensive vehicles will not be feasible in the near future, there is no doubt that the use of aluminum-based materials will increase steadily (Refs. 1–3). One attractive area is to use aluminum alloys as structural materials, and this application depends primarily on forming and joining of aluminum parts. As the major joining technique in auto-body assembly, resistance spot welding is used for joining aluminum parts, as it has been used for steel.

The nonheat-treatable Al-Mg alloys (5000 series) in sheet product form are among the most promising aluminum materials, and among them, AA5754 has been developed especially for the automotive industry. The optimized magnesium content in the alloy assures satisfactory mechanical properties and low susceptibility to stress corrosion cracking. The AA5754 alloy has good formability, good static, impact and fatigue strength and high resistance to pitting and intercrystalline corrosion (Refs. 4, 5), as well as a stable microstructure after exposure in moderate temperatures. The strength of the alloy results from a combination of solid-solution hardening, cold work and grain-size strengthening, as expressed by the Hall-Petch equation. The microstructure of this alloy and resulting features are described in detail by Burger, *et al.* (Ref. 5). Because AA5754 sheet material is annealed and its surface pre-treated, thereby assuring repeatability in resistivity for spot welding, it is generally regarded as a material with "good spot weldability" (Ref. 4). This has been confirmed by a number of publications with positive experimental results for "classical" spot welding (Refs. 6–10), as well as for weld bonding (Refs. 11, 12).

Although it is known that one of the major problems in welding Al alloys is cracking, there is very little information in published literature concerning crack formation in AA5754 or similar alloys during spot welding. Toyota reported solidification failure in the nugget or liquation cracking in the heat-affected zone (HAZ) for one of the 5000 series alloys containing above 5 wt-% Mg (Ref. 13). They observed cracking under a wide range of welding parameters and suggested that preheating or increasing welding time may decrease thermal stresses and therefore decrease cracking tendency. The possibility of cracking was also indirectly implicated in spot welding AA5754 by Thornton, *et al.* (Ref. 10).

Although there is very limited published literature on cracking mechanisms during resistance spot welding, cracking has been studied relatively extensively for arc welding aluminum alloys of various working ranges, and high susceptibility to hot cracking during solidification of the liquid pool has been reported. For instance, Lippold, *et al.* (Ref. 14) investigated hot cracking in two lots of 5083 aluminum alloy (4.28 and 4.78 wt-% Mg, respectively) weldments that were gas tungsten arc (GTA) welded. They observed crack initiation and propagation in either the fusion zone or the HAZ and found that cracking susceptibility depends on the Mg content in the particular alloy and weld orientation relative to the rolling direction of the material. In continuous-wave CO_2 laser beam welding and pulsed Nd:YAG laser welding 5000 Al-Mg alloy series, including AA5754, Jones, *et al.* (Ref. 15), reported fairly low hot-cracking susceptibility. They observed the tendency toward cracking increases with Mg content, reaching a peak value at 2 wt-% Mg; high weld strength and low crack susceptibility were found when Mg content is above 4 wt-%. The maximum cracking tendency in Al-Mg alloys was reported earlier at approximately 3 wt-% Mg (Ref. 16) or 1–2 wt-% Mg (Ref. 17). The observations are consistent with hot-tearing phenomenon in casting of Al alloys (Ref. 18), in accordance with the established fact that the peak of hot-cracking susceptibility of binary alloys is at about one half of maximum solubility of the second component in the solid state.

J. SENKARA AND H. ZHANG are with Department of Mechanical Engineering and Applied Mechanics, University of Michigan, Ann Arbor, Mich. J. SENKARA is on sabbatical leave from Welding Dept., Warsaw University of Technology, Warsaw, Poland.

KEY WORDS

Resistance Spot Welding
Aluminum Alloy
Hot Cracking
Cracking Mechanism
Healing
Heat-Affected Zone
Stress
Strain

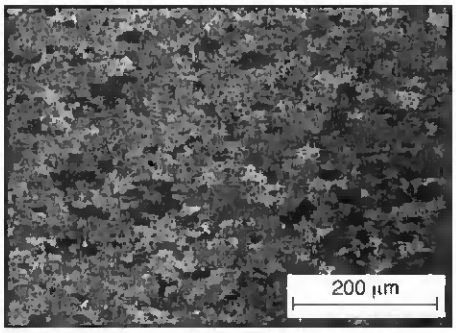

Fig. 1— Microstructure of AA5754 base material used in the experiment.

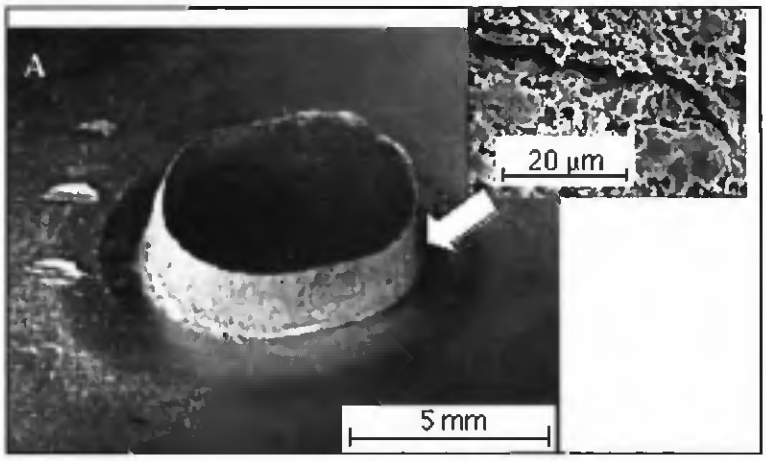

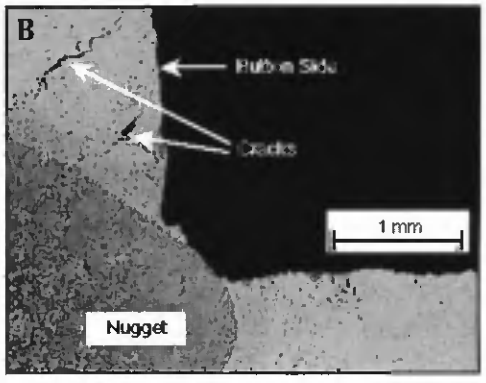

Fig. 2— Appearance of a typical button after peel testing. A — An amplified side view of the button wall; B — cross section of the same button.

It is noteworthy to compare cracking during welding with solidification cracking during casting, although there are differences in the processes. According to the classical works by Pellini and Flemings, hot tearing in casting alloys occurs at the last stage of crystallization (Refs. 18–21), during which solid grains are surrounded by the liquid; such a structure has a very low strength. Tensile stresses and strains, resulting from nonuniform temperature distribution and cooling, may cause material failure. A certain amount of strain is necessary for crack initiation, as pointed out by Pellini (Ref. 19). Hot cracking tendencies in casting increase with grain dimensions, solidus-liquidus gap and solidification shrinkage, which is especially high for Al alloys. The presence of impurities and grain boundary segregation also promote cracking.

The mechanism of hot cracking in welding, similar to that in casting, is based on a theory developed by Borland (Ref. 22) and Prokhorov (Ref. 23). Occurrence of cracking in "coherence temperature range" (Borland's definition) depends on both critical strain and critical strain rate. Hot cracking during welding at elevated, near-solidus temperatures includes failure of welds (solidification cracking) and cracking in the HAZ (liquation cracking) (Ref. 24). Cracking in the HAZ is related to liquation at the grain boundaries of either the secondary phase or low-melting-point impurities, at subsolidus and at supersolidus temperatures of the primary phase. Existing theories of formation and solidification of grain boundary liquid films include equilibrium melting of the vicinity of grain boundaries (Ref. 25), constitutional liquation of secondary phases and the effects of segregation (Refs. 26, 27).

Comparisons of various Al alloys in casting and arc welding revealed the Al-Mg system is second to the Al-Cu system in crack susceptibility among aluminum alloys (Refs. 16, 18, 21, 28), in spite of only a small amount of eutectic formed during solidification (Ref. 16).

The lack of practical information on cracking in spot welded Al-Mg alloys, the increasing use of Al alloys in the automotive industry and the care needed for spot welding aluminum alloys are the driving forces for the study of cracking in resistance spot welding AA5754 sheets. Because single spot welds are rarely used in welded structures, multispot welds were chosen for this investigation. The influence of metallurgical interaction among spot welds and other factors are emphasized to understand the mechanisms of crack initiation and propagation.

Experiments

AA5754 aluminum alloy sheets of 1.6- and 2.0-mm gauges and in 0 temper condition (annealed), produced by Alcan Aluminum Co., were used in all experiments. The sheet surface was pretreated and prelubricated by the producer. The chemical composition specified by the producer, as well as the composition of the sample tested independently, are listed in Table 1. The data show that the tested composition is within the specified range.

The sheets were cut into 350 x 25-mm coupons for multiwelding. Taking into account the small anisotropy of structure and properties reported by Burger, *et al.* (Ref. 5), all coupons were cut out parallel to the rolling direction. Figure 1 shows a typical material microstructure of the base metal. Slightly elongated grains representing Mg in Al solid solution are visible as are precipitates of Al_3Mg_2, (Fe, Mn)Al_6 and silicides.

In this set of experiments, Alcan's domed electrodes were used. Such an electrode has a face diameter of 10 mm, and the radius for the domed face is 50 mm.

Multiwelds were made on the coupons using a medium-frequency (MF) DC welding machine. The welding parameters used were 7 kN electrode force, 3 kA preheat current for 3 cycles (50 ms), 12 cycles (200 ms) of weld delay, 26 kA welding current for 5 cycles (83 ms) and 12 cycles (200 ms) of holding time. The weld pitch was 30 mm. Generally, welds with satisfactory appearance were obtained. Commonly used peel testing confirmed good quality and repeatability of the spot welding process. A regularly shaped, good sized button is shown in Fig. 2A.

Spot welded samples were then sectioned in two perpendicular directions (normal and parallel to the rolling direction) and were ground, polished and structurally investigated to disclose possible internal discontinuities and their natures. Optical and scanning electron microscopy techniques were used, as were energy dispersive X-ray (EDX) and wave dispersive X-ray (WDX) microanalyses. Microhardness was measured across the sectioned weldment using a LECO hardness tester.

Description of Cracks

Despite the normal appearance of a typical button after peeling, an amplified side view of the button wall revealed

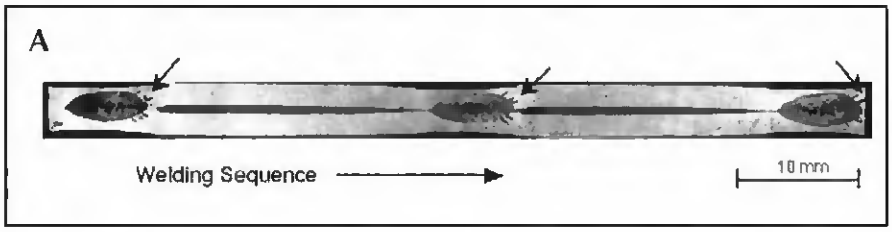

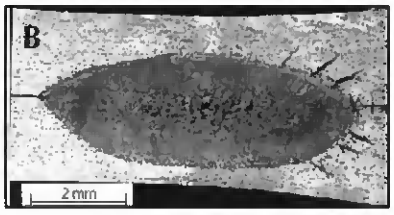

Fig. 3 — Longitudinal cross section of a multispot welded coupon. A — Cracks on the right side of the nuggets; B — one of its nuggets by higher magnification. C — For comparison, the transverse cross section of a neighboring nugget is also presented.

Table 1 — Chemical Composition of AA5754 (Ref. 4) and of the Sheets Tested (in wt-%)

	Mg	Mn	Cu	Fe	Si	Ti	Cr	Zn
Nominal	2.6–3.6	0.5[a]	0.1[a]	0.4[a]	0.4[a]	0.15[a]	0.3[a]	0.2[a]
Tested	3.22	0.25	<0.05	0.19	<0.05	<0.05	<0.05	<0.05

[a] Maximum value.

cracks — Fig. 2A. This was confirmed by optical and scanning electron microscope (SEM) examination of the sectioned specimens (Fig. 2B); these revealed discontinuities of porosity and cracks in the weldments. Although a certain volume of porosity could be seen in the weld nugget on all the cross sections of welded samples, there were no cracks in the nuggets. Optical microscopy inspection, however, revealed many cracks on the sides of nuggets in many specimens. Cracks were all located in the HAZ. In many cases, the gaps of cracks were filled by the base material, which was detectable only after etching. Cracks were found only on one side of the nugget, with respect to welding sequences — Fig. 3. In this case, they are clearly visible from longitudinal cross sections, whereas there are no visible cracks or only very narrow traces of cracks visible in transverse sections.

The appearance of cracks, their locations and their orientations are fairly regular as revealed by the examination of a large number of specimens. The angles between the main axes of cracks and the tangents to the weld interface are similar and are equal to about 70 deg for the specimens examined, as shown by the statistics of the orientations of nearly 70 cracks in Fig. 4.

A photo of higher magnification shows intergranular fracture characteristics — Fig. 5. Cracks initiate in the vicinity of the weld interface in the HAZ and propagate away from the nugget into the base metal. A typical cracking trace is not straight, as shown in Fig. 5. It follows the grain boundaries while keeping the overall outward direction. Some of the cracks tilt slightly toward the faying interface as they propagate. Most of them are wide at their bases and become narrower toward the base material. Wide cracks have tree-like structures, *i.e.*, large trunks (wide opening of cracks at the bottom) formed from fine roots (grain boundaries). Many of them are fully or partially filled — Fig. 6. The failure surface has a dendritic morphology — Fig. 7.

Cracks initiate in a zone where the alloy remained in the solidus-liquidus temperature range during welding at some distance from the weld interface — Fig. 5. A "web" of grain boundaries decorated by precipitation is visible around the zone. Grain boundary failure can be clearly seen near the base of the wide-opening cracks. A typical microstructure of the region in the HAZ close to the nugget and at some distance from cracks is presented in Fig. 8. Precipitates inside the grains and at grain boundaries (intergranular precipitates), where they form chains or even continuous layers, are visible. EDX and WDX analyses revealed an increased amount of Mg in these regions. This is most probably due to an Al_3Mg_2 secondary phase (the presence of which should be about 6% in the Al-Mg3.5 alloy, according to the Al-Mg equilibrium phase diagram [Ref. 29]), which exists in the alloy before welding and serves as the source of liquid at elevated temperature. This was confirmed by X-ray diffraction examination.

The hardness in the nugget, the HAZ — both near and far from cracks — and the base metal were measured, as shown in Fig. 9. Generally, there is no difference in hardness between the nugget, the HAZ and the base AA5754 alloy. The hardness near the crack in the HAZ is somewhat higher than the hardness some distance from it, which may suggest strain hardening. The scatter of the hardness data inside the nugget results from microporosity.

Mechanisms of Cracking and Healing

Cracking and healing in AA5754 have been observed in multiwelded specimens, as demonstrated in previous sections. Although discontinuities such as porosity and cracks inside a nugget may not influence the strength, as suggested by Thornton, *et al.* (Ref. 10), and Michie and Renaud (Ref. 30), the occurrence of cracks outside the nugget as revealed by this study may influence the strength of the welded components; this needs further study. It is therefore necessary to study the mechanisms of cracking and potential structure remediation. Like all other processes of resistance spot welding, the formation, propagation and recovery of cracks involve interactions of metallurgical, thermal and mechanical factors. The influence of these factors is analyzed in the following sections.

Metallurgical Factors

The cracking phenomenon in the HAZ during spot welding of AA5754 described in this study is consistent with the observations in published literature on the susceptibility to cracking of other aluminum alloys containing several percent of magnesium in casting (Ref. 18) and arc welding (Ref. 28). No solidification cracks, however, were observed in the nuggets in the present study, contrary to the observations of Watanabe, *et al.* (Ref. 13).

Intergranular characteristics of cracks in the HAZ and dendritic morphology of failure surfaces, as shown in Figs. 5–7, are typical features of hot cracking and evidence of cracking at elevated temperatures. The dendrite structure inside open cracks proves that liquid had to be present at the moment of crack formation,

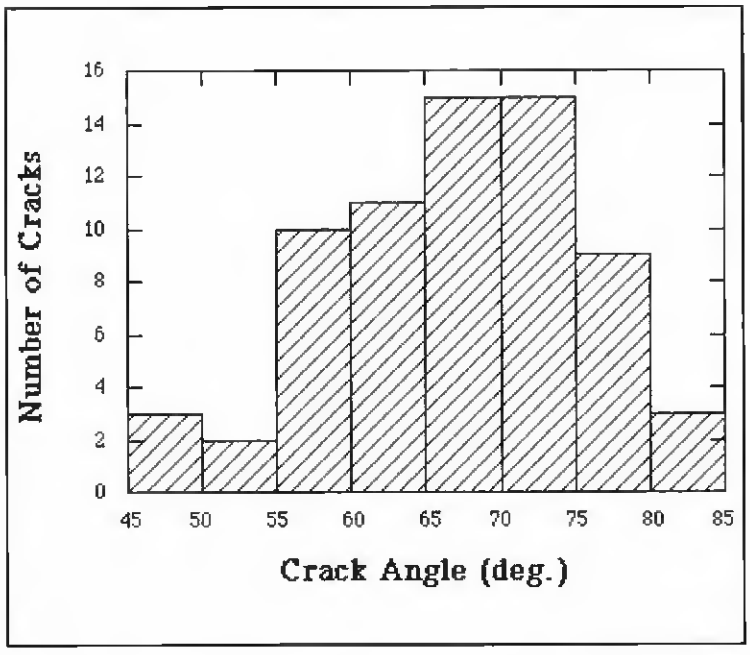

Fig. 4 — Measured crack angles with respect to weld interface.

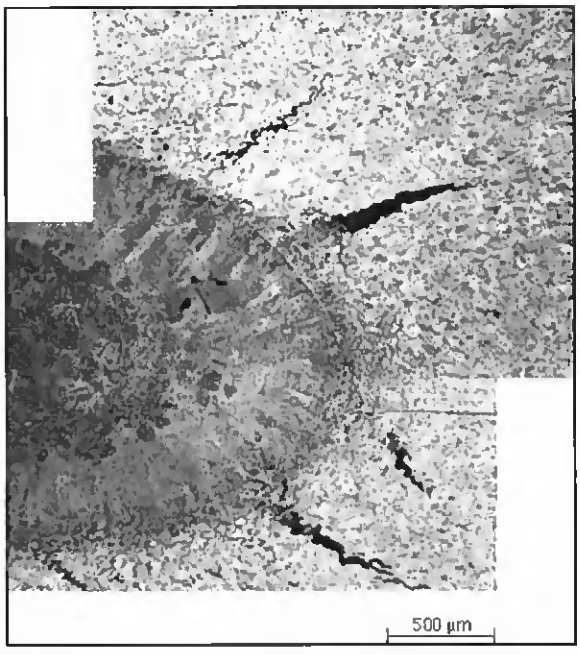

Fig. 5 — A close look at cracks in the HAZ.

and, therefore, it is liquation cracking according to the classification by Hemsworth, *et al.* (Ref. 24). The microporosity visible in some inclusions of the secondary phase serves as additional evidence of the existence of liquid in this part of the HAZ during spot welding.

Generally, there are two possible ways for melting to occur at grain boundaries in the HAZ: at supersolidus temperatures and at subsolidus temperatures. In the heating stage of welding, equilibrium melting of the material near grain boundaries occurs in the part of the HAZ heated to the temperature range between solidus and liquidus (partially melted zone). In addition to partially melting at temperatures above the solidus, liquation of the secondary phase may occur at subsolidus temperatures. During rapid heating, which is a characteristic of resistance spot welding, there is not sufficient time to dissolve the Al_3Mg_2 phase in the α-solution matrix, and inclusions of this phase still exist after the alloy is heated over the solvus line. Al_3Mg_2 inclusions melt in the region (next to the partially melting zone) that experiences maximum temperature above the eutectic point but below the solidus temperature. Existence of liquid below the solidus of AA5754 can also be attributed to other low-temperature melting additions/impurities present in a commercial alloy. The zones around the nugget are schematically shown in Fig. 10. Structures/zones in the HAZ are linked to the equilibrium phase diagram via assumed temperature history during RSW. The dynamic effects in the heating/cooling processes, such as overheating and undercooling, were not investigated in this study due to experimental difficulties, although they may contribute to hot cracking. For instance, the effective solidus temperature during cooling may be lower than the equilibrium solidus temperature because of the high cooling rate in RSW. This effectively enlarges the temperature range in which the material is weak and susceptible to cracking.

As a result of combined supersolidus and subsolidus melting/liquation, large grains in these parts of the HAZ are surrounded by liquid during welding. Nearly continuous films of liquid are formed at grain boundaries — Fig. 8. Therefore, the overall material structure close to the nugget is favorable for crack initiation and growth during the last stage of heating in resistance spot welding Al-Mg alloys.

After the current is switched off, the material cools quickly because of heat transfer through the water-cooled electrodes. The life of transient liquid films at grain boundaries depends on several factors, including the cooling rate and compositional segregation. For AA5754, the difference between equilibrium temperatures of liquidus (915 K), solidus (876 K) and eutectic temperature (723 K) is significant, according to the Al-Mg phase diagram (Ref. 29). Decreases of the solidus and eutectic solidification temperatures can be expected due to kinetic effects during cooling. The coexistence of solid and liquid phases at grain boundaries is then extended in a relatively wide temperature range during the cooling stage.

High heating and cooling rates, as well as a high temperature gradient in the weldment due to the nature of Joule heating, are the thermal characteristics of spot welding. Based on the experiments conducted in this study of welding AA5754, the heating and cooling rates are estimated to be as high as 8000 and 3000 K/s, respectively. Because of this, liquid films at grain boundaries may exist for an extended time at elevated temperatures, as proved by Radhakrishnan and Thompson in their model (Ref. 27). This results from the concentration gradient in the liquid due to rapid solidification, which effectively lowers the solidification temperatures of liquid parts with higher (than equilibrium) Mg concentration.

As described above, metallurgical factors during spot welding of AA5754 create favorable conditions for tearing the structures in the HAZ.

Thermomechanical Factors

Besides the metallurgical effect, thermomechanical factors also play a role in the initiation and subsequent propagation and growth of cracks. This section is devoted to describing the mechanisms of crack formation by qualitative thermal and mechanical analyses using simplified assumptions (because of the complicated mechanical, thermal and metallurgical interactions).

As seen in Fig. 3A, cracks appear on

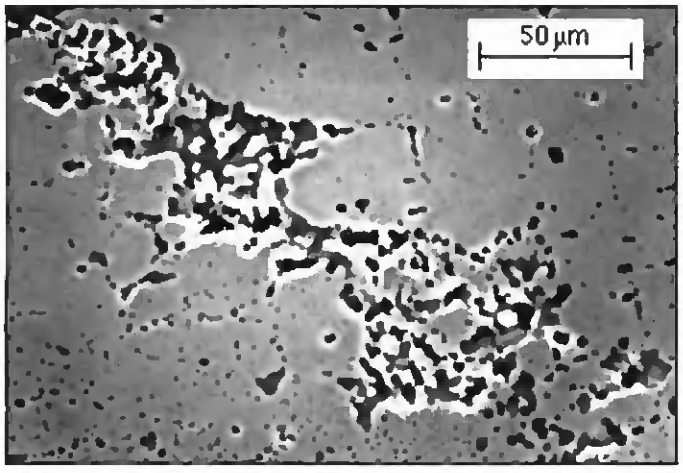

Fig. 6 — An almost fully filled crack.

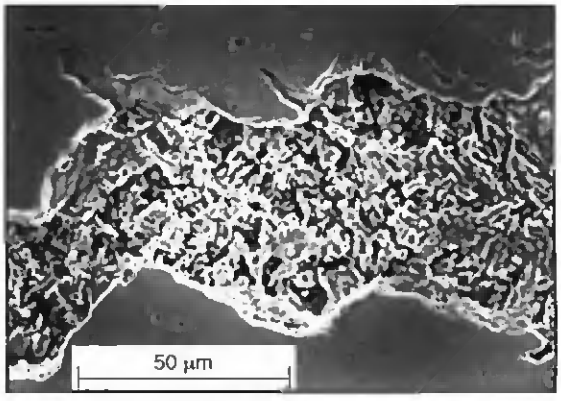

Fig. 7 — Intergranular characters of a crack and dendritic morphology of failure surface.

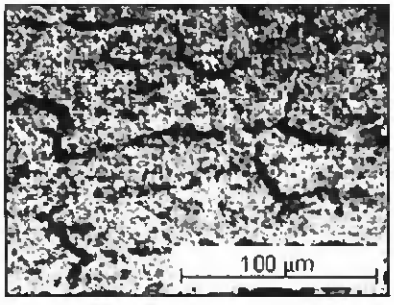

Fig. 8 — Precipitation zone in the HAZ.

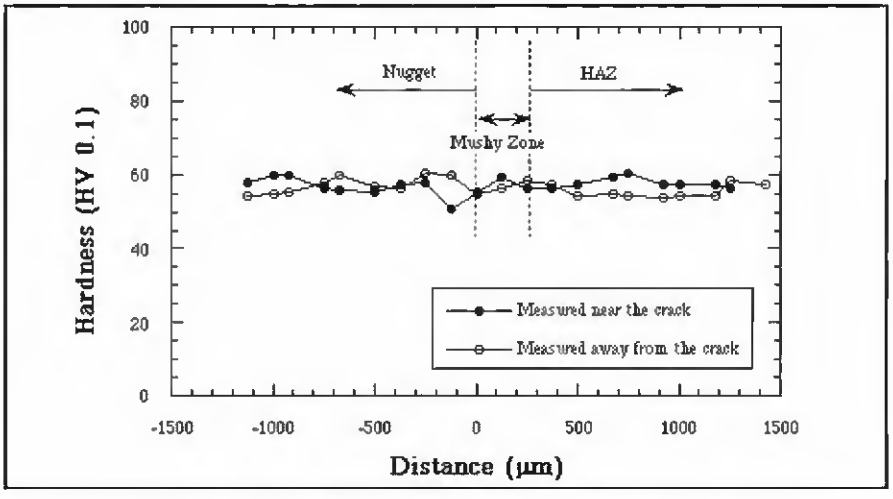

Fig. 9 — Hardness distribution of a spot weldment.

the leading sides of nuggets that coincide with the welding sequence in a multi-spot welded strip. No significant traces of cracking have been found on the trailing sides of the nuggets. Figure 11 shows the outline of a spot weldment (Fig. 3B) that includes workpieces, the nugget and cracks. It is taken from the middle of a multiwelded strip, and the welding sequence is from the left side (Side L) to the right side (Side R). The crack initiation and propagation can be explained based on the physical processes this weld has gone through during welding.

Material Flow

From Fig. 11, it can be seen that the weldment is not symmetric. Specifically, there is no significant deformation near the faying surface (sheet-sheet interface) in the solid phase on Side L, while on Side R there is virtually no separation near the nugget, hut a blunt notch can be seen at a distance of approximately 0.7 mm from the nugget. This unsymmetrical configuration can he seen in all the weldments in Fig. 3A. This phenomenon is directly related to the deformation of the solid phase in the HAZ near the nugget during welding.

The resistance heating during welding expands both the molten metal and the solid phase of the weldment. This expansion is constrained by the electrodes and the work sheets surrounding the weldment. The loading condition on one sheet can be simplified as shown in Fig. 12. On top of the sheet, there is an applied electrode force, simplified as distributed load. There is also a liquid pressure, developed in the nugget, as demonstrated in a previous work by the authors (Ref. 31), inserted on the bottom of the solid phase. The boundary conditions shown in the figure reflect the constraints imposed by the surrounding solid phase. Because of the forces inserted by the electrodes and the liquid nugget, the solid phase between the electrode and the nugget is squeezed in a process similar to a rolling operation. During welding, there is usually a temperature gradient in the solid phase in the HAZ as revealed by a finite element analysis (Ref. 32). The temperature in the solid near the liquid nugget is higher than the temperature farther from it, because that area is constantly cooled by the electrodes. Because of this nonuniform temperature distribution in the weldment, the solid near the liquid nugget tends to expand more than the solid away from the nugget; therefore, there is a tendency toward sheet separation on the sides of the nugget. This separation, however, is not even on the two sides. On Side L, the sheets are confined by the previous weld. No large separation is allowed on this side. The situation is different on Side R. Because there is significantly less constraint on the sheets on this side, which was free during welding, there is very little resistance to sheet separation. Consequently, the solid metal around the liquid nugget and at the faying interface near the nugget on Side R are squeezed out between the electrode, the nugget and

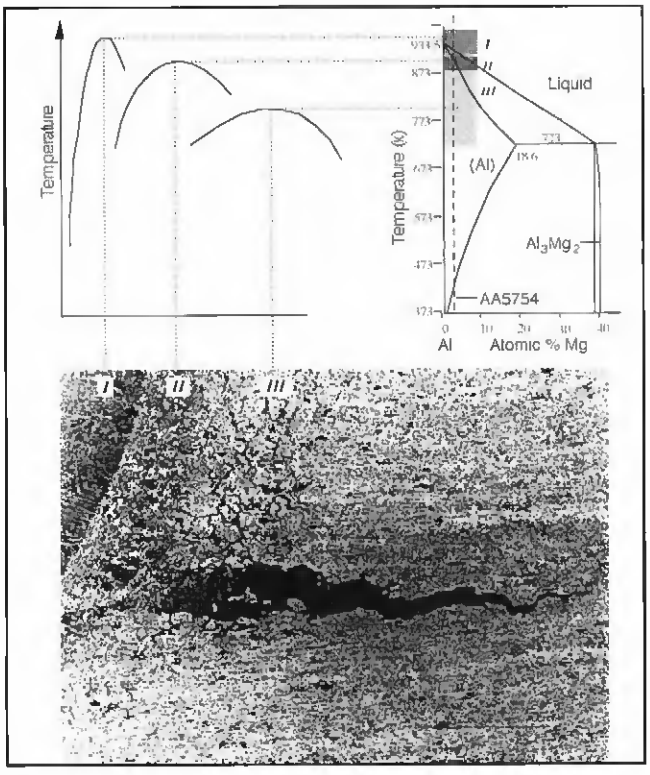

Fig. 10 — Schematic diagram of the links between the equilibrium phase diagram of Al-Mg and the solidified structures after welding through possible temperature history of various zones. Zone I: fusion zone; Zone II: partially molten zone; Zone III: liquation zone.

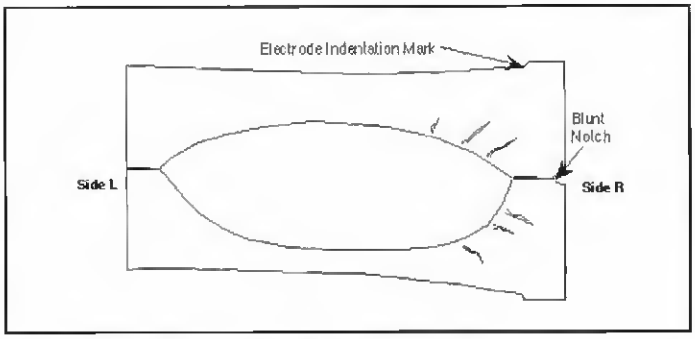

Fig. 11 — Outline of the weldment in Fig. 3B.

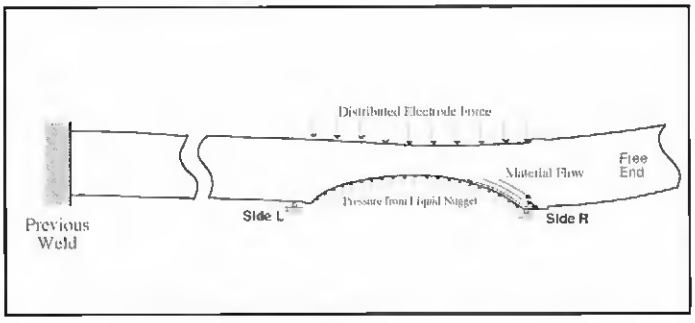

Fig. 12 — Loading and mechanical constraining on a weldment during multiwelding and schematic material flow. Side L is constrained by the previous weld.

the other workpiece, as evidenced by the geometry of the blunt notch and the electrode indentation mark shown in Fig. 11. This material flow is made possible by the high temperature (just below the solidus) field surrounding the liquid nugget, which softens the solid by lowering the yield strength.

Thermal Stress Development

Stresses are developed in the solid during heating and cooling, and they are closely related to the constraining conditions. The solid phase between the electrodes and the liquid nugget tend to expand during heating. Because of the difference in constraint, the stress developed during heating is different on the two sides. Materials near the weld interface tend to expand more than those away from the weld interface. On Side L, large compressive stress is developed in the direction parallel to the weld interface due to constraints from the solid phase of the sheets. Meanwhile, on Side R, there is very little compressive stress buildup in the vicinity of the nugget, because the solid phase can be squeezed out, as shown in the previous section; this effectively releases the stress.

When the current is cut off, heating is terminated and rapid cooling starts. In fact, cooling is provided by the electrodes during the entire period of welding, but the rate is much higher after the electric current is shut off. The cooling rate is so high (very similar to the rate found in a quenching process) that tensile stresses develop in a very short period of time, regardless of their stress states after heating. By superimposing the stress states during heating and cooling, the final stress can be found tensile on Side R, and very little (tensile or compressive) on Side L. The tensile stress on Side R during cooling is directly responsible for crack initiation in the region.

The tensile stress developed during cooling is approximately along the tangent of the isotherm, which is parallel to the weld interface, near the nugget. Therefore, the orientation of the crack is normal to the tangent, or along the temperature gradient.

Stressing Due to Bending

Because of the constraint conditions imposed on one of the sheets as shown in Fig. 12, the workpieces are bent under the electrode force. The stress induced by the electrode force, though, is not the same for the two sides due to uneven constraining conditions. To understand the stress state of the workpiece under electrode force, the workpiece is idealized as a simply supported cantilever beam, with consideration given to constraining conditions and loading, and electrode force is simplified as a uniformly distributed load. The distance between the previously made weld (simulated as a fixed end) and the left side of the weld under consideration is approximately the weld pitch. By a structural mechanics derivation, the distribution of the bending moment in the beam is as depicted in Fig. 13A. It clearly shows that in the solid near the weld interface, compressive stress is developed due to electrode force on Side L, while tensile stress is developed on Side R. Note that the distributed load in Fig. 13A is the resultant of applied electrode force and pressure from the liquid nugget.

The liquid pressure in the nugget, which acts on the opposite side of the worksheet, may relax to a certain extent the bending stress resulting from the electrode force. However, in most cases, the force due to nugget pressure is of less magnitude compared with electrode force, as the applied electrode forces are normally chosen to sufficiently contain the liquid from expulsion. The net tensile stress accelerates cracking when combined with the thermal stresses analyzed in previous sections.

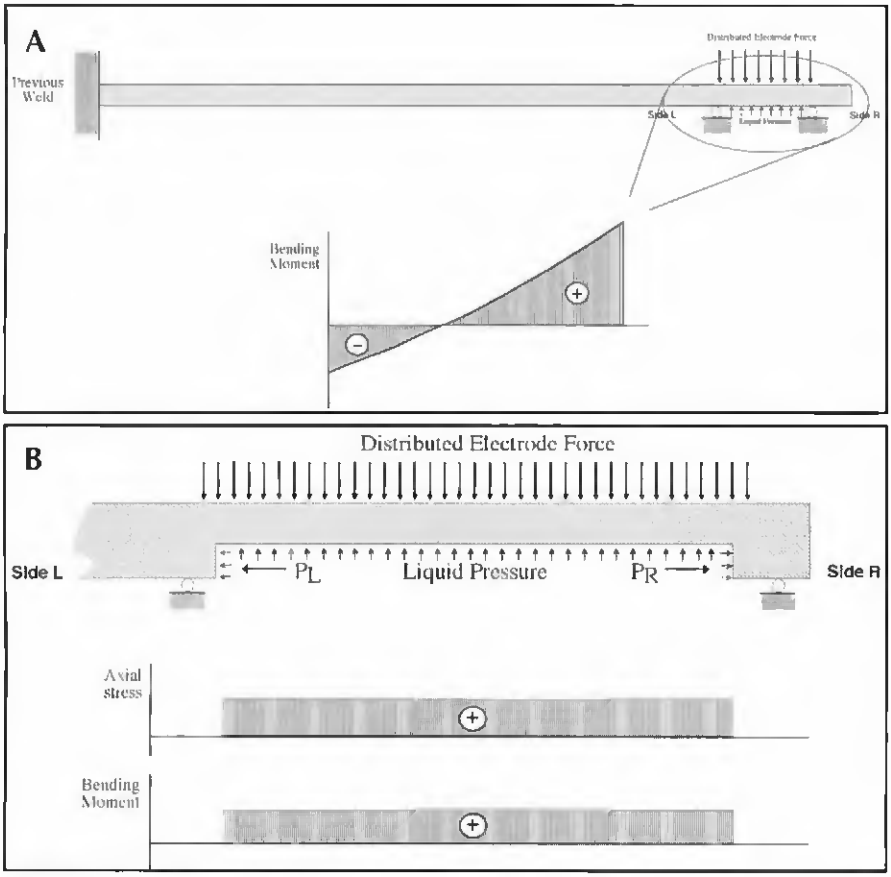

Fig. 13 — Simplified loading and boundary conditions, and resulting bending moment and force, to understand the influence of electrode force (A) and liquid pressure or expulsion (B) on cracking.

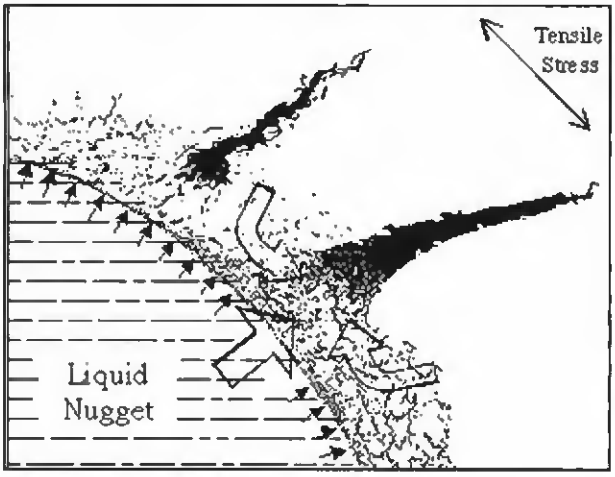

Fig. 14 — Schematic illustration of crack filling mechanisms. Arrows indicate possible paths for liquid being ejected into the crack.

Contribution of Expulsion to Cracking

Expulsion stems from liquid metal pressure (Ref. 31), and its contribution to cracking is mainly mechanical. Expulsion itself is the ejection of liquid metal from the nugget during heating, so it helps material flow. It also increases the tensile stress/strain in the solid. Take Fig. 12 as an example and assume expulsion through Side R as is frequently observed during multispot welding. The liquid metal pressure in the nugget exerts a force to the sides in the direction parallel to the faying interface; this is illustrated in Fig. 13B. The value of forces P_L and P_R can be approximated as liquid pressure multiplied by half of the nugget height. Because of the constraint on Side L, P_L has virtually no influence on the stress and strain in the solid, while P_R induces tensile stress and strain by extending and bending the workpiece — Fig. 13B. Once part of the liquid metal is pushed out, the solid between the electrode and liquid nugget moves inward, adding tensile stress to the region in the solid near the liquid nugget. In addition to tensile stress, expulsion also induces a high strain rate to the solid near the weld interface, because the side wall of the liquid nugget is pushed outward to the side by an extremely high-speed liquid metal ejection under pressure. This high strain rate is detrimental if it falls in the brittle deformation range.

During welding and the subsequent processes, all of the factors, both metallurgical and mechanical, contribute to the formation and propagation of cracks in the HAZ. Because of the complexity and changing nature of the spot welding process, it is impossible to quantitatively identify the contribution of each factor. However, the developed understanding of cracking mechanisms can be used to formulate guidelines for avoiding cracking in resistance spot welding.

Crack Healing Mechanisms

Depending on the stages in which cracks initiate during welding, the crack gaps may or may not be filled. The most likely mechanism for filling the cracks is leading liquid metal from the nugget into cracks during welding. This is supported by a WDX analysis that revealed slightly higher Mg content inside the filled area, but no significant difference between the chemical composition of the material filling the gaps and that of the base metal.

If a crack exists during heating it may be easily filled because of high pressure inside the liquid nugget (Ref. 31), and then the structure is "healed." As shown in Fig. 14, under tension, the material near the nugget may open up and form cracks. A zone of solid with low strength, or even a partially molten zone, exists between the root of the cracks and the nugget. Because of the high liquid pressure in the nugget, which can be more than 100 MPa (estimated by the authors in Ref. 31), the liquid in the nugget may be pushed at a very high speed through the mushy zone into the opening and may follow the extension of cracks. Another source of filling material is the liquid eutectic existing at the grain boundaries near the weld interface. But this eutectic alone is not sufficient to fill cracking gaps because of its limited amount (6% estimated for AA5754 according to equilibrium phase diagram). The healing process is not always possible because it depends on the resistance of the mushy zone to liquid metal flow/penetration. If a crack is formed during heating, or close to the nugget, it has a high chance of being filled. A crack that forms when cooling starts, or that initi-

ates far from the weld interface, has less chance to be filled; or it can be only partially filled. Further study is needed to understand how welding parameters influence cracking in aluminum alloys. Based on the cracking mechanisms in multispot welding AA5754 discussed in this paper, methods are proposed to minimize/eliminate cracking, as described in Ref. 33. The conclusions drawn here can be used in practice to prevent cracking and, therefore, to make aluminum alloys more suitable for structural use.

Conclusions

Cracking in resistance welding is a complicated subject because of the complex nature of spot welding. The analyses of cracking mechanisms presented in this paper are attempts to provide an understanding of cracking phenomenon and to prevent it from happening. The following conclusions can be drawn from this study:

1) Aluminum Alloy AA5754 was found susceptible to cracking during resistance multispot welding according to the welding sequences under certain circumstances.

2) Intergranular characteristics of failure surfaces and their dendritic morphology indicate the formation of cracks at near-solidus temperatures and also the possibility of crack filling by liquid metal.

3) Metallurgical analysis revealed favorable conditions for cracking in the HAZ during RSW as the result of a liquid layer formation at grain boundaries due to melting and liquation.

4) A thermomechanical analysis showed that local stress and strain in the HAZ from the unconstrained side of a weldment became tensile during welding and may overcome weakened material strengths at elevated temperatures.

5) The phenomena of material flow and thermal expansion/shrinking, as well as expulsion in the process of multispot welding, contribute to the development of stresses in the solid phase (in the HAZ) during heating and cooling.

6) There is a high probability of instantly filling open cracks with highly pressurized liquid from the nugget, if cracks form and propagate before the electric current is shut off. This instantaneous filling is a characteristic of spot welding aluminum alloys, which has not been observed in other welding or cracking systems. A separate preliminary experimental investigation showed that cracking has no significant influence on static tensile-shear strength.

Acknowledgments

The authors greatly acknowledge D. Boomer (Alcan Aluminum Co.) for helping with specimen preparation and M. Kimchi (Edison Welding Institute) for providing facilities for part of the structural analyses.

References

1. Cole, G. S., and Sherman, A. M. 1995. Lightweight materials for automotive applications. *Materials Characterization*, 1: 3–9.

2. Irving, B. 1995. Building tomorrow's automobiles. *Welding Journal* 74(8): 29–34.

3. Osterman, F. 1993. *Aluminum Materials Technology for Automobile Construction.* Mechanical Engineering Publications Ltd. London.

4. *Automotive Sheet Specification.* Alcan Rolled Products Co., Feb. 1994.

5. Burger, G. B., Gupta, A. K., Jeffrey, P. W., and Lloyd, D. J. 1995. Microstructural control of aluminum sheet used in automotive applications. *Materials Characterization* 35:23–34.

6. Keay, B. B. 1992. Welding of aluminum for automotive body assembly. *AWS Sheet Metal Welding Conference V*, Detroit, Mich., Paper No. D4.

7. Newton, C. J., Browne, D. J., Thornton, M. C., Boomer, D. R., and Keay, B. F. 1994. The fundamentals of resistance spot welding aluminum. *Proc. AWS Sheet Metal Welding Conference VI*, Detroit, Mich., Paper No. E2.

8. Hao, M., Osman, K. A., Boomer, D. R., and Newton, C. J. 1994. Development in characterization of resistance spot welding of aluminum. *Proceedings of 75th AWS Welding Conference*, Philadelphia, Pa., Paper No. 94089.

9. Browne, D., Newton, C., and Boomer, D. 1995. Optimization and validation of a model to predict the spot weldability parameter lobes for aluminum automotive body sheet. *Proceedings of International Body Engineering Conference*, Advanced Technologies and Processes Section, Detroit, Mich., pp. 100–106.

10. Thornton, P. H., Krause, A. R., and Davies, R. G. 1996. The aluminum spot weld. *Welding Journal* 75(3): 101-s to 108-s.

11. McGregor, I. J., Gao, I., Sheasby, P., and Wilson, I. 1995. Weld-bonding: a joining technology for aluminum structured vehicles. *Proceedings of International Body Engineering Conference*, Automotive Body Materials Section, Detroit, Mich., pp. 76–84.

12. Wang, P. C., Chisholm, S. K., Banas, G., and Lawrence, F. V. 1995. The role of failure mode, resistance spot weld and adhesive on the fatigue behavior of weld-bonded aluminum. *Welding Journal* 72(2): 41-s to 47-s.

13. Watanabe, G., and Tachikawa, H. 1995. Behavior of cracking formed in aluminum alloy sheets on spot welding. 48th Annual Assembly of IIW, Stockholm. IIW Doc. No. III-1041-95.

14. Lippold, J. C., Nippes, E. F., and Savage, W. F. 1977. An investigation of hot cracking in 5083-O aluminum alloy weldments. *Welding Journal* 56(6): 171-s to 178-s.

15. Jones, J. A., Yoon, J. W., Riches, S. T., and Wallach, E. R. 1994. Improved mechanical properties for laser welded automotive aluminum alloy sheets. *Proc. AWS Sheet Metal Welding Conference VI*, Detroit, Mich., Paper No. B2.

16. Cross, C. E., Tack, W. T., Loechel, L. W., and Kramer, L. S. 1990. Aluminum weldability and hot tearing theory. *Weldability of Materials*, pp. 275–282, and R. A. Patterson, K. W. Mahin, eds., ASM International, Materials Park, Ohio.

17. Anik, S., and Dorn, L. 1991. Metal physical processes during welding — weldability of aluminum alloys. *Welding Research Abroad* 37: 41–44.

18. Rosenberg, R. A., Flemings, M. C., and Taylor, H. F. 1960. Nonferrous binary alloys hot tearing. *Transactions of the American Foundrymen's Society* 68: 518–528.

19. Pellini, W. S. 1952. Strain theory of hot tearing. *The Foundry* 80: 125–133.

20. Bishop, H. F., Ackerlind, C. G., and Pellini, W. S. 1957. Investigation of metallurgical and mechanical effects in the development of hot tearing. *Transactions of the American Foundrymen's Society* 65: 247–258.

21. Flemings, M. C., Uram, S. Z., and Taylor, H. F. 1960. Solidification of aluminum castings. *Transactions of the American Foundrymen's Society* 68: 670–684.

22. Borland, J. C. 1961. Suggested explanation of hot cracking in mild and low alloy steel welds. *British Welding Journal* 8: 526–540.

23. Prokhorov, N. N. 1968. Theorie und verfahren zum bestimmen der technologischen festigkeit von metallen beim schweissen. *Schweisstechnik* 19: 8–11.

24. Hemsworth, B., Boniszewski, T., and Eaton, N. F. 1969. Classification and definition of high temperature welding cracks in alloys. *Metallurgy*, Feb., pp. 5–12.

25. Thompson, R. G. 1990. Inter-granular liquation effects on weldability. *Weldability of Materials*, pp. 57–63, R. A. Patterson and K. W. Mahin, eds., ASM International, Materials Park, Ohio.

26. Brooks, J. A. 1990. Weld microsegregation: modeling and segregation effects on weld performance. *Weldability of Materials*: 41–47, R. A. Patterson and K. W. Mahin, eds., ASM International, Materials Park, Ohio.

27. Randhakrishnan, B., and Thompson, R. G. 1992. A model for the formation and solidification of grain boundary liquid in the heat-affected zone (HAZ) of welds. *Metallurgical Transactions A* 23A: 1783–1799.

28. Cross, C. E., and Olson, D. L. 1986. Hot tearing model to assess aluminum weldability. *Aluminum Alloys — Their Physical and Mechanical Properties* III: 1869–1875, ELMA5, E. A. Starke and T. H. Sanders, eds.

29. T. B. Massalski, ed. 1990. *Binary Alloy Phase Diagrams*, 2nd Ed., p. 130. ASM International, Materials Park, Ohio.

30. Michie, K. J., and Renaud, S. T. 1996. Aluminum resistance spot welding: how weld defects affect joint integrity. Proc. *AWS Sheet Metal Welding Conference VII*, Detroit, Mich., Paper No. B5.

31. Senkara, J., Zhang, H., and Hu, S. J. 1998. Expulsion prediction in resistance spot welding, submitted to *Welding Journal*.

32. Zhang, H., Huang, Y., and Hu, S. J. 1996. Nugget growth in spot welding of steel and aluminum. *Proc. AWS Sheet Metal Welding Conference VII*, Detroit, Mich., Paper No. B3.

33. Zhang, H., Senkara, J., and Wu, X. 2000. Suppressing cracking in RSW AA5754 aluminum alloys by mechanical means, submitted to *Journal of Engineering Manufacture.*